Hyperparameter-Free RFF Based Post-Distorter for OTFS VLC System

Anupma Sharma, *Graduate Student Member, IEEE*, Rangeet Mitra, Ondrej Krejcar, Kwonhue Choi, *Senior Member, IEEE*, Michal Dobrovolny, and Vimal Bhatia, *Senior Member, IEEE*

***Abstract*—Visible light communication (VLC) has emerged as an eco-friendly and low-cost technology for the next-generation communication systems. However, for VLC systems, existing works report performance degradation due to light-emitting-diode (LED) non-linearity, multipath and relative mobility between the transmitter and the receiver. Additionally, multipath and user-mobility introduce inter-symbol-interference (ISI) and frequency-domain spreading which degrades the performance of VLC systems. For such scenarios, orthogonal time frequency space (OTFS) modulation is well-known to jointly addresses impairments due to multipath and user-mobility. To mitigate the distortions due to LED non-linearity, recently reproducing kernel Hilbert space (RKHS)-based random Fourier feature (RFF) techniques have emerged which alleviate the dependence on learning a dictionary and, outperforms classical polynomial based techniques. However, performance of these techniques is sensitive to the choice of kernel-width. Thus, for the OTFS systems impaired by LED non-linearity, this manuscript proposes a hyperparameter-free RFF-based post-distorter, under finite-memory budget without the need of explicitly tuning kernel-width for best performance. Analytical bounds for the bit-error-rate (BER) performance of the proposed post-distorter are presented, and validated via simulations over realistic VLC channels. From the results it is verified that the proposed receiver achieves better BER performance over uncompensated scenario and classical baseline polynomial based technique.**

Manuscript received 24 March 2023; accepted 26 March 2023. Date of publication 31 March 2023; date of current version 10 April 2023. This work was supported in part by the MeitY's 13(23)/2020-CC&BT Scheme, in part by the University of Hradec Kralove, Faculty of Informatics and Management, Czech Republic under Grant UHK FIM-SPEV-2023-2102, in part by the NSP of Slovak Republic, and in part by NRF funded by Korea Government (MSIT) under Grant 2021R1A2C1010370. *(Corresponding author: Kwonhue Choi.)*

Anupma Sharma is with the Department of Electrical Engineering, Indian Institute of Technology Indore, Indore 453552, India (e-mail: phd1901202007@iiti.ac.in).

Rangeet Mitra is with the School of Technology, Woxsen University, Hyderabad, Telangana 502345, India (e-mail: rangeetmi86@gmail.com).

Ondrej Krejcar is with the Faculty of Informatics and Management, University of Hradec Kralove, 50003 Hradec Kralove, Czech Republic, also with the Malaysia Japan International Institute of Technology (MJIIT), Universiti Teknologi Malaysia, Kuala Lumpur 54100, Malaysia, and also with the University of Zilina, 010 26 Zilina, Slovakia (e-mail: ondrej.krejcar@uhk.cz).

Kwonhue Choi is with the Department of Information and Communication Engineering, Yeungnam University, Gyeongsan 38541, South Korea (e-mail: gonew@yu.ac.kr).

Michal Dobrovolny is with the Faculty of Informatics and Management, Center for Basic and Applied Research, University of Hradec Kralove, 50003 Hradec Kralove, Czech Republic, and also with the Department of Electrical Engineering, Center for Advanced Electronics, Indian Institute of Technology Indore, Indore 453552, India (e-mail: xdobro4@gmail.com).

Vimal Bhatia is with the Department of Electrical Engineering, Indian Institute of Technology Indore, Indore 453552, India, also with the Faculty of Informatics and Management, Center for Basic and Applied Research, University of Hradec Kralove, 50003 Hradec Kralove, Czech Republic, and also with the University of Zilina, 010 26 Zilina, Slovakia (e-mail: vbhatia@iiti.ac.in).

Digital Object Identifier 10.1109/JPHOT.2023.3263560

***Index Terms*—Visible light communication (VLC), orthogonal time frequency space (OTFS), random Fourier feature (RFF), bit error rate (BER).**

I. Introduction

VISIBLE light communication (VLC), has emerged as a viable green supplement for traditional radio frequency (RF) communication due to its unique features, such as, wide licence free spectrum, low electromagnetic interference (EMI), higher security, and low cost [1]. For these reasons, VLC has emerged as an upcoming technology for the future 5G and beyond communication systems [2]. In a typical VLC system, the energy-efficient luminaries, such as, light emitting diode (LED) is used as transmitter by intensity modulation to achieve the dual goal of data-transmission and illumination.

Although promising, performance of a VLC system is known to degrade due to the following two major factors: (1) non-linear characteristic of LED [3] that adds an equivalent additive distortion at the receiver, and (2) user-mobility and inter-symbol-interference (ISI) which leads to time-domain and frequency-domain spreading respectively [4]. Conventional modulation schemes for VLC such as, optical-orthogonal frequency division multiplexing (O-OFDM) are capable of mitigating ISI due to time-domain dispersion caused by multipath reflections [5]. For O-OFDM based VLC system, various pre-distorters [3] and post-distorters [6] are used to mitigate the effect of LED non-linearity. Further, user mobility leads to variations in VLC channel-gains, that in-turn, leads to lowering of instantaneous signal-to-noise ratio (SNR) [4]. To jointly mitigate impairments due to user mobility and multipath dispersion, recently, orthogonal time frequency space (OTFS) modulation technique has been proposed [7].

There are primarily two ways to mitigate the effect of LED non-linearity i.e. by using pre-distorters and post-distorters. Pre-distortion techniques are known to outperform static inversion, however, it requires perfect feedback of the channel state information (CSI) from the receiver to the transmitter in a closed loop. To alleviate the need for precise feedback, authors in [8], [9], [10] substituted pre-distorters with open loop post-distorters based on Volterra and Hammerstein polynomials. However, the Volterra (ex. Volterra least mean square (VLMS)) and Hammerstein based approaches have high computational complexity and suffer from modelling impairments due to truncation of polynomial series. Thus, due to their universal representation, open loop reproducing kernel Hilbert

space (RKHS) based post-distortion methods have been proposed recently. RKHS based approaches are computationally simple and provide superior bit error rate (BER) performance. Among the existing RKHS based post-distortion techniques, the kernel least mean square (KLMS) and kernel minimum symbol error rate (KMSER) are the most popular. RKHS based post-distorter based on KLMS/KMSER algorithm delivers better performance over polynomial series based post-distorters. However, KLMS/KMSER based approaches rely on growing dictionary of data sets, which is difficult to implement practically. Furthermore, the feature function of Gaussian kernel allows for approximation as random Fourier feature (RFF). In [6], authors have presented superior performance of RFF based least minimum symbol error-rate post-distorter in RKHS over IEEE 802.15r1 PAN VLC channels. Also, the authors in [11] have proposed an RFF based KMSER decision feedback equalizer (DFE) for VLC. However, the performance of RKHS based techniques whether dictionary-based or RFF is highly sensitive to the choice of kernel-width parameter. Estimating the appropriate kernel-width for convergence adds to the computational complexity. From [12], it is noted that kernel-width sampled from inverse-gamma distribution has same error as compared to the kernel-width obtained by brute-force trial. Building on this observation, in this paper hyperparameter-free RFF based post-distorter for OTFS VLC System is proposed.

Since the first paper on OTFS [7], OTFS has shown remarkable improvement in the performance as compared to OFDM over both dynamic and static channels for RF communication. However, application of RF based systems are greatly limited for beyond 5G applications due to the following factors: severe electromagnetic-interference (EMI) in industrial radio-hostile environments, ambient noise, multipath effect, Doppler effect due to relative motion between the receiver and the transmitter, and power limitation [13]. VLC-OTFS based system proposed by authors in [14], is a viable solution to mitigate the limitations of RF-OTFS based systems. Extensive research is required to exploit VLC-OTFS systems in the beyond 5G communication system. Authors in [15], [16], have shown that over static and mobile multipath channels for indoor VLC environment, OTFS demonstrates superior performance than the conventional OFDM technique in terms of BER. In [17], [18], [19], authors have proposed multi, quad and dual LED-OTFS systems which do not require Hermitian symmetry or direct current (DC) bias operations for indoor VLC environment and analyzed better BER performance of OTFS over OFDM. Authors in [20] have proposed DCO-OTFS based relay-assisted VLC system to enhance the spectral efficiency. In [21], authors have proposed 2D encryption algorithm for a secure DCO-OTFS VLC system. In practice, the LED has non-linear characteristic that affects the performance of a VLC system which can play an important role in the deployment. Hence, the impact of non-linear LED is considered in this work which is not available in [14], [15], [16], [17], [18], [19], [20], [21]. To enhance such VLC links and for generic impairment-mitigation, hyperparameter-free RFF based post-distorters have emerged as promising solution [11] for the OTFS VLC system.

Contributions: In this paper, for the first time in the literature, we propose an algorithm for performance improvement of an OTFS based VLC system with user mobility. This paper proposes RFF based post-distortion for OTFS over VLC systems with user-mobility and time-domain dispersion. The salient contributions of this letter are:

- This paper proposes OTFS for VLC system impaired by both multipath and user mobility. For our studies, channel impulse response (CIR) measurements generated using Zemax software for realistic trajectories are considered [4].
- To mitigate distortions due to LED non-linearity the hyperparameter-free least square-RFF (LS-RFF) based post-distorter is proposed for OTFS, and its BER performance is evaluated.
- A lower bound on the BER of the proposed RFF based post-distorter is obtained analytically and validated via computer simulations over non-linear VLC channels with varying severity levels.

Simulations are performed over a realistic mobile-multipath VLC channel to validate the proposed post-distorter.

Notations: Scalars, vectors, and matrices are denoted as a, $\mathbf{a}$, and $\mathbf{A}$, respectively. $\mathbf{a}_i$ and $\mathbf{A}_{i,j}$ represent the ith element of vector $\mathbf{a}$ and (i,j)th element of matrix $\mathbf{A}$. The set of matrices with dimension $K \times L$ having each entry from the complex plane is denoted by $\mathbb{C}^{K\times L}$. Let $\mathbf{A} = \text{circ}[\mathbf{A}_0, \ldots, \mathbf{A}_{L-1}] \in \mathbb{C}^{KL\times KL}$ represent the circulant matrix. Transpose of a vector $(\cdot)$ is denoted by $(\cdot)^T$. The $\otimes$ denote the convolution operator. $\mathcal{N}(\mu, \sigma^2)$ denote the Gaussian distribution with mean μ and variance σ^2.

II. System Model

In this section, the system model for the VLC-OTFS system impaired by LED non-linearity and the multipath channel is described in Fig. 1. The number of symbols transmitted per frame is $N_s = UV$, where U and V are the number of symbols and the number of sub-carriers, respectively. The transmitted binary phase shift keying (BPSK) symbols mapped in delay-Doppler domain are represented as $\mathbf{x} \in \mathbb{C}^{N_s\times 1}$. Two dimensional (2D) inverse symplectic fast Fourier transform (ISFFT) is applied on input BPSK modulated vector $\mathbf{x}$ to transform it into time-frequency domain such that

$$\mathbf{X}_{v,u} = \sum_{l=0}^{U-1}\sum_{k=0}^{V-1} \mathbf{x}_{l,k} e^{-j2\pi(\frac{ul}{U} - \frac{vk}{V})}. \tag{1}$$

In the second step, Heisenberg transform on the output of the ISFFT $\mathbf{X}$ is applied to transform it into time-domain

$$\tilde{\mathbf{x}}(t) = \sum_{u=0}^{U-1}\sum_{v=0}^{V-1} \mathbf{X}_{v,u} e^{j2\pi u\Delta f(t-vT)} g_x(t-vT), \tag{2}$$

where $g_x(t)$ is the transmitted pulse. In the time-frequency domain sampling is done at intervals T and Δf, respectively, to obtain a 2D lattice $\Lambda = (vT, u\Delta f)$, where $v = 0, \ldots, V-1$, and $u = 0, \ldots, U-1$. After OTFS modulation, a cyclic prefix (CP) of length $(C_p - 1)$ is affixed to the output before transmitting, where C_p is the number of channel paths. After adding CP, the DC bias is added to the transmitted signal to bring the LEDs into the forward bias (operating) region. Next, symbols are transmitted through LED with non-linear characteristics. As LEDs have amplitude-to-amplitude (AM/AM) modelling,

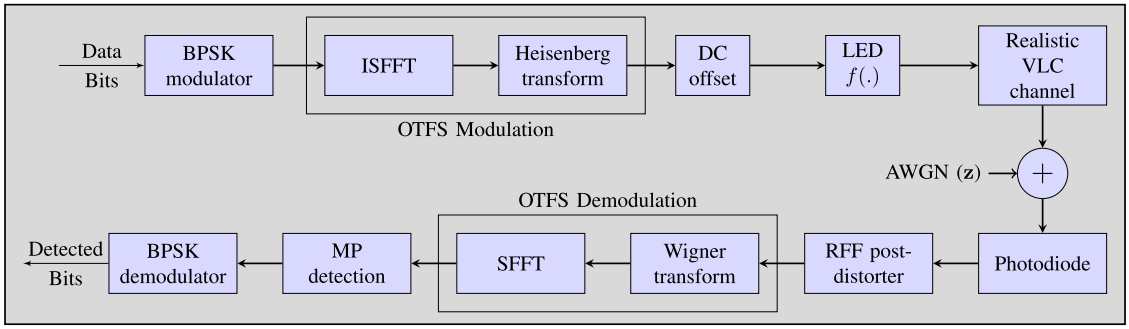

Fig. 1. Block diagram of the considered system model.

non-linear characteristics of LED is modelled by Rapp's model as follows

$$f(\tilde{\mathbf{x}}) = \frac{\tilde{\mathbf{x}}}{\left(1 + \left(\frac{\tilde{\mathbf{x}}}{i_{sat}}\right)^{2k_f}\right)^{\frac{1}{2k_f}}}, \tag{3}$$

where i_{sat} is the saturation current of the LED and k_f is the knee factor which controls smoothness of the transition from the linear to the saturation region. The output is transmitted over mobile-multipath VLC channel $\mathbf{H}(\tau, \nu)$ [4], defined as

$$\mathbf{H}(\tau, \nu) = \sum_{i=1}^{C_p} h_i \delta(\tau - \tau_i)\, \delta(\nu - \nu_i), \tag{4}$$

where ν_i, τ_i, h_i are Doppler shift, delay and channel gain, respectively, for the ith cluster, and $\delta(\cdot)$ denotes the Dirac delta function.

Due to LED non-linearity, the bit vector transmitted is denoted by $f(\tilde{\mathbf{x}})$. Therefore, the received signal at the photodiode after discarding the CP can be written as [7]

$$\mathbf{r}(t) = \int_{\nu}\int_{\tau} \mathbf{H}(\tau, \nu) f(\tilde{\mathbf{x}}(t-\tau)) e^{j2\pi\nu(t-\tau)} d\tau d\nu + \mathbf{z}(t),$$
$$\mathbf{r} = \mathbf{H} \otimes f(\tilde{\mathbf{x}}) + \mathbf{z}, \tag{5}$$

where $\mathbf{z} \in \mathbb{C}^{N_s \times 1}$ is independent and identically distributed (i.i.d.) additive white Gaussian noise (AWGN) whose tth entry is defined as $\mathbf{z}_t \sim \mathcal{CN}(0, \sigma_z^2)$. At the receiver, the symbols received by the photodiode are in the time-domain $\mathbf{r}(t)$ and are mapped back to the information domain after post distortion. First, the time-domain symbols are mapped back to time-frequency domain $\mathbf{Y}_{v,u}$ by applying Wigner transform

$$\mathbf{Y}_{v,u} = \int \mathbf{r}(\tau) r_x^*(\tau - t) e^{-j2\pi f(t-\tau)} d\tau, \tag{6}$$

where r_x^* is the conjugate of the received pulse r_x. Receiving and transmitting pulses g_x and r_x are ideal such that they satisfy the property of biorthogonality. Then symplectic fast Fourier transform (SFFT) is applied on output of Wigner transform $\mathbf{Y}_{v,u}$ [7] to transform signal mapped in the time-frequency domain to the information domain.

$$\mathbf{y}_{l,k} = \frac{1}{\sqrt{UV}} \sum_{v=0}^{V-1} \sum_{u=0}^{U-1} \mathbf{Y}_{v,u} e^{-j2\pi\left(\frac{ul}{U} - \frac{vk}{V}\right)}. \tag{7}$$

Therefore, the input-output relation of the considered system model in the information domain, i.e. delay-Doppler domain, can be equated as

$$\mathbf{y} = \mathbf{H}_{\mathbf{eff}}\mathbf{x} + \tilde{\mathbf{z}}, \tag{8}$$

where $\mathbf{H}_{\mathbf{eff}}$ is the effective channel matrix in information domain, and $\tilde{\mathbf{z}}$ is the noise which has the same statistical properties of $\mathbf{z}$. In the next section, a hyperparameter-free RFF based least squares (LS) based post-distorter is proposed for the mitigation of transmit-side LED non-linearity, and its performance bounds are derived.

III. Hyperparameter-Free LS-RFF

In this section, we propose a hyperparameter-free LS-RFF based post-distorter for mitigating transmit-side non-linearity for the considered OTFS VLC system. Owing to the superior performance of RFF based technique in RKHS over the classical polynomial based techniques such as VLMS and advantage of finite-memory budget over other RKHS based methods, we propose a hyperparameter-free based approach to alleviate the need for estimating the hyperparameter i.e. kernel-width. Notably, the hyperparameter-free RFF are viable for mitigation of arbitrary transmit-side non-linearity without the knowledge of hyperparameters like kernel-width or the explicit nature of the underlying non-linearity.

We consider reference waveforms, $\mathbf{r}_{ref}$ at the receiver corresponding to the pre-determined pilots $\tilde{\mathbf{x}}_{ref}$. Further, without loss of generality, the first N_{tr} subcarriers of $\mathbf{r}_{ref}$ are used for training, the same is denoted as $\mathbf{r}_{ref} < 1 : N_{tr} >$, corresponding to pilots $\tilde{\mathbf{x}}_{ref} < 1 : N_{tr} >$. Further, we denote the augmented regressors by concatenation of the real and imaginary parts as follows

$$\mathbf{r}^c_{ref} < 1 : N_{tr} >$$
$$= [\text{real}(\mathbf{r}_{ref} < 1 : N_{tr} >); \text{imag}(\mathbf{r}_{ref} < 1 : N_{tr} >)], \tag{9}$$

and

$$\tilde{\mathbf{x}}^c_{ref} < 1 : N_{tr} >$$
$$= [\text{real}(\tilde{\mathbf{x}}_{ref} < 1 : N_{tr} >); \text{imag}(\tilde{\mathbf{x}}_{ref} < 1 : N_{tr} >)]. \tag{10}$$

Further, the regressors are mapped to RKHS by the hyperparameter-free RFF, which, for n_G RFFs, is denoted as

follows

$$\mathbf{\Phi}(\mathbf{r}^c_{ref} < 1 : N_{tr} >) = \sqrt{\frac{2}{n_G}} \cos\left(\text{diag}[\boldsymbol{\zeta}]\mathbf{A}\mathbf{r}^c_{ref} < 1 : N_{tr} > +\mathbf{b}\right), \tag{11}$$

where the vectors $\boldsymbol{\zeta}$ is drawn from a Gamma distribution, $\mathbf{\Gamma}[\alpha, \beta]$, and mapping coefficients $\mathbf{A}$ and $\mathbf{b}$ are drawn respectively from a zero mean normal distribution with unit variance, and uniformly distributed random variable in the interval $[0, 2\pi]$. Further, the parameters of the Gamma distribution can be initialized as follows

$$\alpha = \frac{UV}{2}, \tag{12}$$

$$\beta = \epsilon, \tag{13}$$

where ϵ is an arbitrarily small constant. Using these hyperparameter free RFFs, the estimate of the autocorrelation matrix, $\hat{\mathbf{R}}_{\mathbf{\Phi}}$, is expressed as follows

$$\hat{\mathbf{R}}_{\mathbf{\Phi}} = \frac{1}{N_{tr}} \sum_{m=1}^{N_{tr}} \mathbf{\Phi}(\mathbf{r}^c_{ref} < 1 : N_{tr} >)\mathbf{\Phi}(\mathbf{r}^c_{ref} < 1 : N_{tr} >)^T. \tag{14}$$

and the cross covariance is expressed as

$$\hat{\mathbf{r}}_{\mathbf{\Phi}} = \frac{1}{N_{tr}} \sum_{m=1}^{N_{tr}} (\tilde{\mathbf{x}}^c_{ref} < 1 : N_{tr} >)\mathbf{\Phi}(\mathbf{r}^c_{ref} < 1 : N_{tr} >). \tag{15}$$

which allows for the following estimate of the equalizer weights,

$$\mathbf{w} = \hat{\mathbf{R}}^{-1}_{\mathbf{\Phi}} \hat{\mathbf{r}}_{\mathbf{\Phi}}. \tag{16}$$

which, in-turn, allows for the following unwarped/equalized estimate, $\mathbf{r}^c_{unwarped}$, as follows

$$\mathbf{r}^c_{unwarped} = \mathbf{w}^T \mathbf{\Phi}(\mathbf{r}^c_{ref}). \tag{17}$$

The MSE of the proposed receiver, σ_e^2, can be given as follows

$$\sigma_e^2 = 1 - \hat{\mathbf{r}}^T_{\mathbf{\Phi}} \hat{\mathbf{R}}^{-1}_{\mathbf{\Phi}} \hat{\mathbf{r}}_{\mathbf{\Phi}}. \tag{18}$$

which allows for the following the SNR

$$\gamma = \frac{1}{\sigma_e^2 + \sigma_z^2}. \tag{19}$$

which, in turn, results in the following lower bound for BER [22],

$$\text{BER} \geq \frac{UV - 1}{2^{UV}} Q\left(\sqrt{2\gamma}\right). \tag{20}$$

Putting the value of γ from (19), finally we get lower bound of BER as

$$\text{BER} \geq \frac{N_s - 1}{2^{N_s}} Q\left(\sqrt{\frac{2}{\sigma_e^2 + \sigma_z^2}}\right). \tag{21}$$

The accuracy of the proposed post-distorter can be validated in Fig. 2. The accuracy of the model can be estimated as

$$\text{Accuracy} = \frac{\text{Total number of correct estimations}}{\text{Total number of bits transmitted}} \times 100, \tag{22}$$

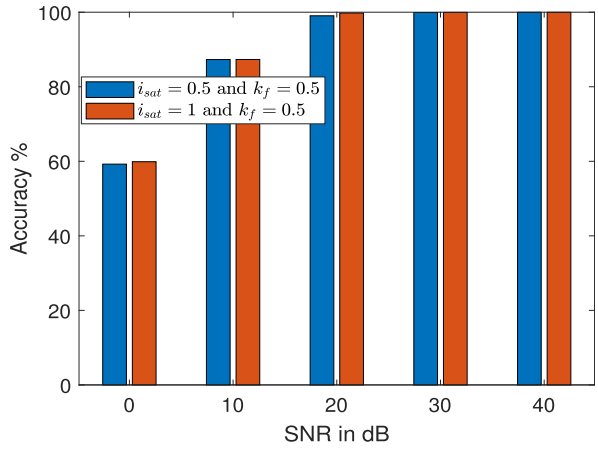

Fig. 2. Accuracy of the proposed post-distorter for both the considered scenarios i.e. $k_f = 0.5$, and $i_{sat} = 1$, 2) $k_f = 0.5$, and $i_{sat} = 0.5$.

TABLE I
ACCURACY OF PROPOSED POST-DISTORTER IN PERCENTAGE

SNR	**Case 1:** $k_f = 0.5$**, and** $i_{sat} = 1$	**Case 2:** $k_f = 0.5$**, and** $i_{sat} = 0.5$
0 dB	59.89	59.24
10 dB	87.32	87.3
20 dB	99.78	99.04
30 dB	99.96	99.92
40 dB	99.99	99.99

TABLE II
SIMULATION PARAMETERS

Parameters	**Specifications**
Number of symbols transmitted per frame (N_s)	2048
Number of subcarriers (V)	1024
Knee factor (k_f) [25]	0.5
Saturation current of LED (i_{sat})[25]	0.5,1
α	1024
β	10^{-3}
Number of training pilots (N_{tr})	100

From Table I, it is observed that for SNR = 0 dB in both Case-1 where $k_f = 0.5$, and $i_{sat} = 1$, and Case-2 where $k_f = 0.5$, and $i_{sat} = 0.5$, the accuracy of the proposed model is $\sim$59%. However, as the SNR is increased to 10 dB the accuracy is enhanced to 87.32% for Case-1 and 87.3% for Case-2. On further increasing the SNR, the proposed model achieves an accuracy of more than 99%.

IV. MESSAGE PASSING DETECTOR

In this Section, the message passing (MP) detection algorithm for VLC is described. The total number of non-zero elements out of N_s in each row and column of $\mathbf{H_{eff}}$ given in (8) are S, where $S < C_p$. Let $\mathcal{U}_b$ and $\mathcal{V}_d$ be the sets of position of non-zero values in the bth row and dth column of $\mathbf{H_{eff}}$, respectively such that $|\mathcal{U}_b| = |\mathcal{V}_d| = S$.

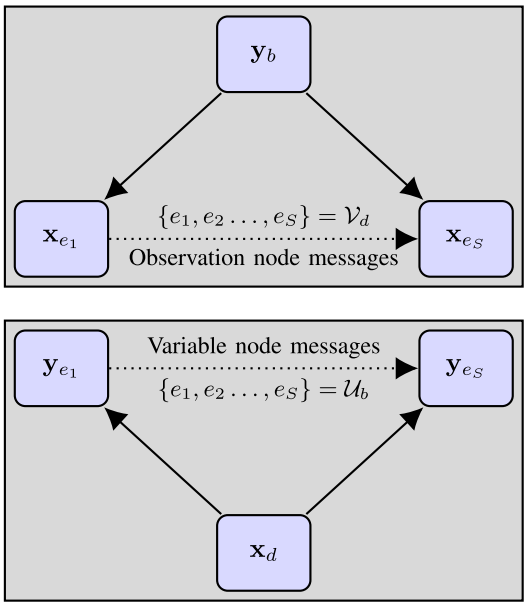

Fig. 3. Messages in the factor graph.

Based on (8), we have modelled the system such that there are N_s variable nodes corresponding to $\mathbf{x}$. Similarly, corresponding to $\mathbf{y}$, there are N_s observation nodes [14], [23], [24]. In the factor graph shown in Fig. 3, the observation node $\mathbf{x}_d$ is connected to the set of variable nodes $\{\mathbf{y}_b, b \in \mathcal{V}_d\}$. Similarly, the variable node $\mathbf{y}_b$ is connected to the set of observation nodes $\mathbf{x}_d, d \in \mathcal{U}_b\}$.

The joint maximum aposteriori probability (MAP) detection rule for estimation of the transmitted information symbols from the received symbols is defined as

$$\hat{\mathbf{x}} = \arg \max_{x \in \mathbb{A}^{N_s \times 1}} \Pr(\mathbf{x}|\mathbf{y}, \mathbf{H_{eff}}). \tag{23}$$

Symbol-by-symbol MAP detection rule is considered for $0 \leq d \leq N_s - 1$,

$$\hat{\mathbf{x}}_d = \arg \max_{a_j \in \mathbb{A}} \Pr(\mathbf{x}_d = a_j|\mathbf{y}, \mathbf{H_{eff}}) \tag{24}$$

$$= \arg \max_{a_j \in \mathbb{A}} \frac{1}{|\mathbb{A}|} \Pr(\mathbf{y}|\mathbf{x}_d = a_j, \mathbf{H_{eff}}). \tag{25}$$

Assume the probability of transmitting all the information symbols $a_j \in \mathbb{A}$ is the same. Also, $\mathbf{x}$ and $\mathbf{y}$ are independent of each other.

$$\hat{\mathbf{x}}_d \approx \arg \max_{a_j \in \mathbb{A}} \prod_{e \in \mathcal{U}_b} \Pr(\mathbf{y}_b|\mathbf{x}_d = a_j, \mathbf{H_{eff}}). \tag{26}$$

In MP algorithm, mean and variance of the interference-plus-noise terms (ϱ_{bd}) are transmitted as messages from observation nodes $\mathbf{y}_b$ for $b \in \mathcal{V}_d$ to variable nodes $\mathbf{x}_d$ for each $d = 0, \ldots, N_s - 1$. The probability mass function of the alphabets in $\mathbb{A}$ is defined as

$$\mathbf{p}_{db} = \{p_{db}(a_j)|a_j \in \mathbb{A}\}. \tag{27}$$

The steps in Algorithm 1 are detailed below. First initialize the iteration index $i = 1$ and $\mathbf{p}_{db}^0 = \frac{1}{\mathbb{k}\mathbb{A}\mathbb{k}}$ for $d = \{0, \ldots, N_s - 1\}$ and $d \in \mathcal{U}_b$. Then, messages are passed to the variable nodes $\mathbf{x}_d$ from the observation nodes $\mathbf{y}_b$. Thus, the message passed has a Gaussian probability density function (pdf) which is computed as

Algorithm 1: MP algorithm for detection of OTFS symbols.

% Input:
$\mathbf{y}$ (estimated signal vector after post-distortion and OTFS demodulation) and $\mathbf{H_{eff}}$ (effective channel matrix)
% Initialization:
Choose pmf $\mathbf{p}_{db}^{(0)} = \frac{1}{\mathbb{k}\mathbb{A}\mathbb{k}}$ for $d = \{0, \ldots, N_s - 1\}$ and $d \in \mathcal{U}_b$, $i_{\max}$
% Computation:
for $i = 1; i < i_{\max}; i++$
- Compute means $(\mu_{b,d}^{(i)})$ and variances $(\sigma_{b,d}^{(i)2})$ of interference-plus-noise term $\varrho_{b,d}^i$ using $\mathbf{p}_{db}^{(i-1)}$ and pass them through observation nodes to variable nodes as messages.
- Variable node update $\mathbf{p}_{db}^{(i)}$ using the message received and passing it to the observation node.
- Update the decision on the information symbol transmitted.
- Increment i till maximum iteration i.e. $i_{\max}$ is reached.

end for
% Output:
$\hat{\mathbf{x}}_d$ (signal vector detected).

$$\mathbf{y}_b = \sum_{e \in \mathcal{U}_b} \mathbf{x}_d \mathbf{H_{eff}}_{b,d} + \tilde{\mathbf{z}} \tag{28}$$

$$= \mathbf{x}_d \mathbf{H_{eff}}_{b,d} + \sum_{e \in \mathcal{U}_b, e \neq d} \mathbf{x}_e \mathbf{H_{eff}}_{b,e} + \tilde{\mathbf{z}} \tag{29}$$

$$= \mathbf{x}_d \mathbf{H_{eff}}_{b,d} + \varrho_{bd} \tag{30}$$

where ϱ_{bd} is the interference-plus-noise term and $\mathbf{H_{eff}}_{b,d}$ is the element in the bth row and the dth column of $\mathbf{H_{eff}}$. As the considered noise is Gaussian, ϱ_{bd} can also be approximated as a Gaussian random variable with mean and variance denoted by $\mu_{bd}^{(i)}$, and $\sigma_{bd}^{(i)2}$ respectively. The transmitted symbols are presumed to be i.i.d. and independent of noise. Variable nodes send messages to the observation nodes. The new message obtained from $\mathbf{x}_d$ to $\mathbf{y}_b$ carries the probability mass function (pmf) vector $\mathbf{p}_{db}^{(i)}$ defined as

$$p_{db}^{(i)}(a_j) = \Delta \cdot \hat{p}_{db}^{(i)}(a_j) + (1 - \Delta) \cdot p_{db}^{(i-1)}(a_j), \tag{31}$$

where $\Delta \in (0, 1]$ is defined as the damping factor.

$$\hat{p}_{db}^{(i)}(a_j) \propto \prod_{e \in \mathcal{U}_b, e \neq d} \Pr(\mathbf{y}_e|\mathbf{x}_d = a_j, \mathbf{H_{eff}}), \tag{32}$$

The final decision on the transmitted symbols is thus,

$$\hat{\mathbf{x}}_d = \arg \max_{a_j \in \mathbb{A}} p_d(a_j), \quad d \in \{0, \ldots, N_s - 1\} \tag{33}$$

where

$$p_d(a_j) = \prod_{e \in \mathcal{U}_b} (\mathbf{y}_e|\mathbf{x}_d = a_j, \mathbf{H_{eff}}). \tag{34}$$

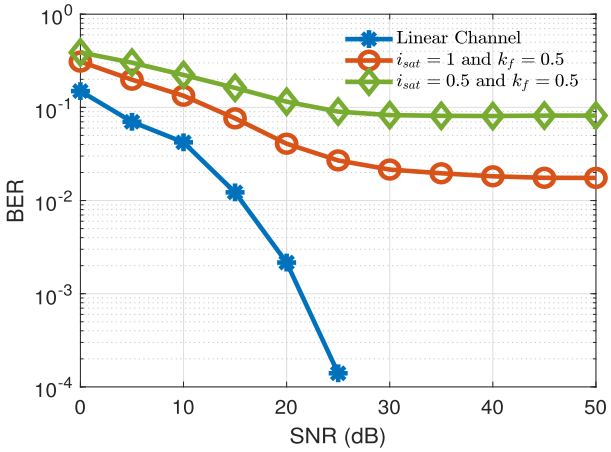

Fig. 4. BER performance comparison for OTFS for linear channel and non-linear channel for $k_f = 0.5$, and $i_{sat} = 1, 0.5$.

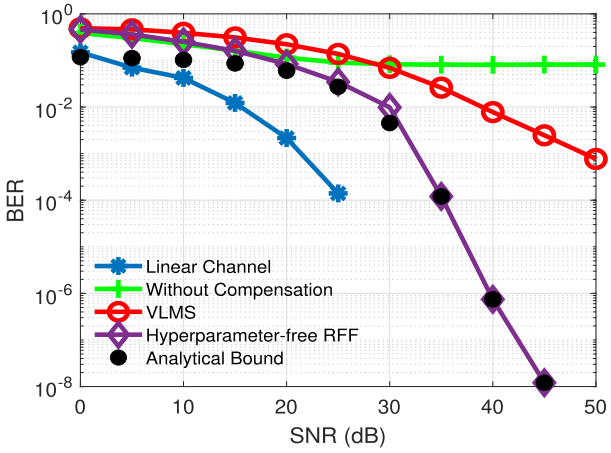

Fig. 5. BER performance comparison for OTFS for the linear channel, non-linear channel, and with hyperparameter free LS-RFF based compensation for $k_f = 0.5$, and $i_{sat} = 1$.

V. Simulation Results

In this section, simulations are presented for validating the proposed hyperparameter-free RFF based receiver. The simulation parameters are summarized in Table I. A non-stationary channel for VLC is considered using a temporal evolution of CIRs, which is obtained by ray tracing using Zemax software [4]. To generalize the performance of the proposed post-distorter, we have considered two cases for non-linearity:

Case-1: $i_{sat} = 1$ and $k_f = 0.5$
Case-2: $i_{sat} = 0.5$ and $k_f = 0.5$

The BER performance of both cases is compared with the linear channel as shown in Fig. 4. The green curve is for the most severe case, i.e. Case-2, and the red curve is for the less severe case, i.e. Case-1. From Fig. 4, the degradation in the BER performance of the proposed OTFS-VLC system after considering LED non-linearity can be observed.

For the proposed detector, the results shown in Fig. 5 indicate a considerable improvement in the BER performance compared

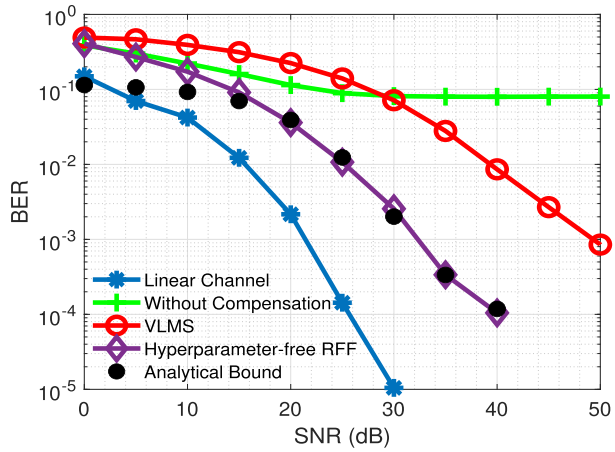

Fig. 6. BER performance comparison for OTFS for the linear channel, non-linear channel, and with hyperparameter free LS-RFF based compensation for $k_f = 0.5$, and $i_{sat} = 0.5$.

to the compensation by VLMS and uncompensated scenario. Also, 2nd order truncated VLMS based post-distorter gives better performance than the uncompensated scenario owing to the non-linear approximation. Furthermore, it is observed that there is a gap between the performances of the proposed hyperparameter-free RFF based detector and the BER performance corresponding to the linear channel. Notably, this gap is quantified in (18) in terms of SNR, which is further mapped via (20) to account for the degradation in the BER performance of the proposed receiver. These analytical results are validated in Fig. 5 considering $k_f = 0.5$, $i_{sat} = 1$, which indicate a close overlap with the analytical results in (18–20).

In Fig. 6, similar results are obtained for a more severe non-linearity with $k_f = 0.5$, $i_{sat} = 0.5$, and compared to the case in Fig. 5, interestingly, similar BER performance is achieved, which reconfirms that the proposed hyperparameter-free RFF based receiver is best suitable for the considered VLC-OTFS system compared to VLMS based receiver. For both cases, the performance of the proposed post-distorter is validated with the analytical results obtained. From Figs. 5 and 6, it is observed that the hyperparameter-free LS-RFF and analytical bound curves overlap in the high SNR regime. Also, the complexity of the proposed receiver is of the order $O(n_G^2)$, which is similar to the existing low-complexity methods of post-distortion, which requires hyperparameter tuning such as RFF-KRLS [6].

VI. Conclusion

In this paper, a hyperparameter-free RFF based receiver was proposed for OTFS to mitigate transmit side device non-linearity. Further, analytical bounds for the performance of the proposed receiver are presented, which were validated via computer simulations over VLC channels with user-mobility. The close overlap of the analytical BER with the simulated BER verifies the analytical contributions of this paper. The results obtained establish robustness of the proposed RFF based post-distortion for the mitigation of transmit side non-linearity for OTFS VLC based system with user-mobility.

REFERENCES

[1] H. Haas, "LiFi: Conceptions, misconceptions and opportunities," in *Proc. IEEE Photon. Conf.*, 2016, pp. 680–681.

[2] S. Ali et al., "6G white paper on machine learning in wireless communication networks," 2020, *arXiv:2004.13875*.

[3] R. Mitra and V. Bhatia, "Chebyshev polynomial-based adaptive predistorter for nonlinear LED compensation in VLC," *IEEE Photon. Technol. Lett.*, vol. 28, no. 10, pp. 1053–1056, May 2016.

[4] K. Reddy Sekhar, F. Miramirkhani, R. Mitra, and A. C. Turlapaty, "Generic BER analysis of VLC channels impaired by 3D user-mobility and imperfect CSI," *IEEE Commun. Lett.*, vol. 25, no. 7, pp. 2319–2323, Jul. 2021.

[5] J. Armstrong, "OFDM for optical communications," *J. Lightw. Technol.*, vol. 27, no. 3, pp. 189–204, Feb. 2009.

[6] R. Mitra, S. Jain, and V. Bhatia, "Least minimum symbol error rate based post-distortion for VLC using random Fourier features," *IEEE Commun. Lett.*, vol. 24, no. 4, pp. 830–834, Apr. 2020.

[7] R. Hadani et al., "Orthogonal time frequency space modulation," in *Proc. IEEE Wireless Commun. Netw. Conf.*, 2017, pp. 1–6.

[8] G. Stepniak, J. Siuzdak, and P. Zwierko, "Compensation of a VLC phosphorescent white LED nonlinearity by means of Volterra DFE," *IEEE Photon. Technol. Lett.*, vol. 25, no. 16, pp. 1597–1600, Aug. 2013.

[9] H. Qian, S. J. Yao, S. Z. Cai, and T. Zhou, "Adaptive postdistortion for nonlinear LEDs in visible light communications," *IEEE Photon. J.*, vol. 6, no. 4, pp. 1–8, Aug. 2014.

[10] Y. Wang, L. Tao, X. Huang, J. Shi, and N. Chi, "Enhanced performance of a high-speed WDM CAP 64 VLC system employing Volterra series-based nonlinear equalizer," *IEEE Photon. J.*, vol. 7, no. 3, pp. 1–7, Jun. 2015.

[11] R. Mitra, G. Kaddoum, and V. Bhatia, "Hyperparameter-free transmit-nonlinearity mitigation using a kernel-width sampling technique," *IEEE Trans. Commun.*, vol. 69, no. 4, pp. 2613–2627, Apr. 2021.

[12] J. B. Oliva, K. A. Dubey, A. G. Wilson, B. Póczos, J. G. Schneider, and E. P. Xing, "Bayesian nonparametric kernel-learning," in *Proc. Int. Conf. Artif. Intell. Statist.*, 2015, pp. 1078–1086.

[13] L. U. Khan, "Visible light communication: Applications, architecture, standardization and research challenges," *Digit. Commun. Netw.*, vol. 3, no. 2, pp. 78–88, 2017.

[14] A. Sharma, S. Jain, R. Mitra, and V. Bhatia, "Performance analysis of OTFS over multipath channels for visible light communication," in *Proc. Int. Conf. Commun., Signal Process., Appl.*, 2021, pp. 1–6.

[15] A. Sharma, S. Jain, R. Mitra, and V. Bhatia, "Performance analysis of OTFS over mobile multipath channels for visible light communication," in *Proc. IEEE Region 10 Conf.*, 2020, pp. 490–495.

[16] J. Zhong, J. Zhou, W. Liu, and J. Qin, "Orthogonal time-frequency multiplexing with 2D Hermitian symmetry for optical-wireless communications," *IEEE Photon. J.*, vol. 12, no. 2, pp. 1–10, Apr. 2020.

[17] S. Sinha and A. Chockalingam, "Multi-LED transmission schemes using OTFS modulation in visible light communication," in *Proc. IEEE 95th Veh. Technol. Conf.*, 2022, pp. 1–6.

[18] S. Sinha and A. Chockalingam, "Quad-LED OTFS modulation in indoor visible light communication systems," in *Proc. IEEE Glob. Commun. Conf.*, 2021, pp. 1–6.

[19] S. Sinha and A. Chockalingam, "OTFS modulation in Dual-LED indoor visible light communication systems," in *Proc. IEEE Veh. Technol. Conf.*, 2021, pp. 1–7.

[20] D. Zheng, H. Zhang, and J. Song, "DCO-OTFS-based full-duplex relay-assisted visible light communications," *Opt. Exp.*, vol. 29, no. 25, pp. 41323–41332, Dec. 2021.

[21] J. Zhong, J. Zhou, S. Gao, and W. Liu, "Secure orthogonal time-frequency multiplexing with two-dimensional encryption for optical-wireless communications," *Chin. Opt. Lett.*, vol. 19, no. 11, 2021, Art. no. 050603.

[22] G. D. Surabhi, R. M. Augustine, and A. Chockalingam, "On the diversity of uncoded OTFS modulation in doubly-dispersive channels," *IEEE Trans. Wireless Commun.*, vol. 18, no. 6, pp. 3049–3063, Jun. 2019.

[23] P. Raviteja, K. T. Phan, Y. Hong, and E. Viterbo, "Interference cancellation and iterative detection for orthogonal time frequency space modulation," *IEEE Trans. Wireless Commun.*, vol. 17, no. 10, pp. 6501–6515, Oct. 2018.

[24] P. Raviteja, E. Viterbo, and Y. Hong, "OTFS performance on static multipath channels," *IEEE Wireless Commun. Lett.*, vol. 8, no. 3, pp. 745–748, Jun. 2019.

[25] H. Elgala, R. Mesleh, and H. Haas, "An LED model for intensity-modulated optical communication systems," *IEEE Photon. Technol. Lett.*, vol. 22, no. 11, pp. 835–837, Jun. 2010.